LES in a Concentric Annular Pipe: Analysis of Mesh Sensitivity and Wall Pressure Fluctuations

Saptarshi Bhattacharjee, Guillaume Ricciardi, Stéphane Viazzo

LES in a Concentric Annular Pipe: Analysis of Mesh Sensitivity and Wall Pressure Fluctuations

S. Bhattacharjee, G. Ricciardi and S. Viazzo

1 Introduction

Annular pipe flows have varied application in the domains of nuclear reactors, heat exchangers, drilling operations in oil industry etc. The first part of the paper (Sect. 2) presents a comparison of large eddy simulations (LES) of turbulent flow in a concentric annular pipe for 5 different mesh resolutions. Results are compared with benchmark DNS data. The second part (Sect. 3) presents its interesting application of pipe flow in the nuclear field. Inside a pressurized water nuclear reactor (PWR) core, flow-induced vibrations due to spacer grids can cause damage to the structure. Understanding this behavior is a challenge. Here the effect of a 'simplified'circular spacer grid on the vortex induced vibrations of the pipe is investigated. LES was performed with the CFD code Trio_U [9] which uses a hybrid finite volume based finite element approach [1]. Simulations were carried out on the Airain and Curie supercomputers at the Computing Center for Research and Technology (CCRT), Bruyères-le-Châtel, France [2].

S. Bhattacharjee (✉) · G. Ricciardi
French Alternative Energies and Atomic Energy Commission (CEA)-Cadarache Center,
DEN/DTN/STCP/LHC, 13108 St Paul lez Durance Cedex, France
e-mail: saptarshi.bhattacharjee@outlook.com

G. Ricciardi
e-mail: guillaume.ricciardi@cea.fr

S. Bhattacharjee · S. Viazzo
Laboratoire de Mécanique, Modélisation et Procédés, Propres (M2P2),
UMR7340 CNRS, Aix-Marseille Université, Centrale Marseille, 13451 Marseille Cedex, France
e-mail: stephane.viazzo@univ-amu.fr

2 Mesh Sensitivity Analysis for LES in a Concentric Annular Pipe

The outer and inner diameters of the pipe were 60 mm and 30 mm respectively. The radius ratio, i.e., the ratio between the inner and outer radii was 0.5. Water flowed through the pipe in axial direction. A schematic diagram is shown in Fig. 1. The hydraulic diameter, defined as $HD = 4A_{flow}/P_{wet}$, was 0.03 m where A_{flow} is the surface area of duct cross-section and P_{wet} is the wetted perimeter. The bulk velocity was 0.298 m/s. Reynolds number based on the bulk velocity and hydraulic diameter was 8900. The length of the domain was 0.24 m, i.e., 8 times hydraulic diameter.

Fully structured tetrahedral meshes were generated with Gmsh [4] and Trio_U's internal meshing tool. The grid was more refined near the boundary in radial direction to study the near-wall behavior (Fig. 2). It was uniform in axial and azimuthal directions. Five different mesh resolutions were considered. Table 1 shows the number of grid points as well as the grid resolution in wall units in each direction for each simulation. Figure 3a–f illustrate the stretching of the tetrahedral elements relative to each other.

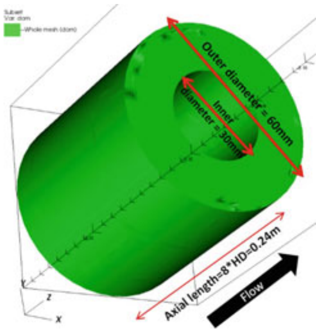

Fig. 1 Schematic diagram of the pipe

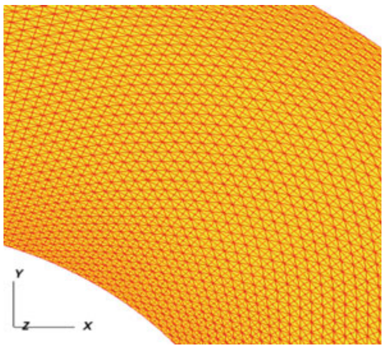

Fig. 2 Non-uniform grid spacing on the radial plane

Table 1 Grid resolution in wall units for 5 different cases

Case	Number of grid points (N_r, N_θ, N_z)	Δ_r^+	Δ_θ^+	Δ_z^+	Elements (in millions)	CPU time (in hours)
C1 (Coarse)	(25, 80, 120)	7.7	9.2	15.3	1.3	4140
C2 (Coarse)	(25, 160, 120)	8.8	5.3	17.6	2.7	9315
F1 (Fine)	(73, 160, 480)	1.3	5.1	2.4	33	74980
F2 (Fine)	(73, 320, 240)	1.3	2.7	4.9	33	111780
UF (Ultra-fine)	(73, 640, 120)	1.3	1.3	9.6	33	74980

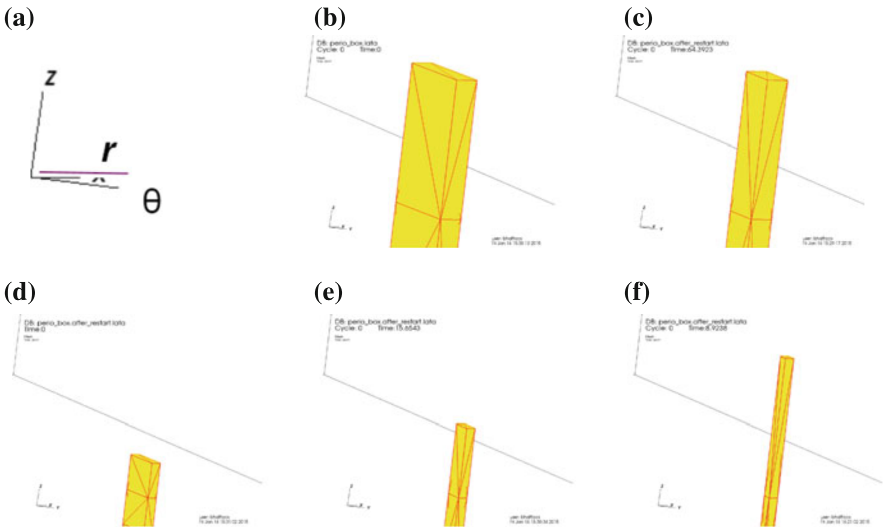

Fig. 3 **a** Axes, **b** C1 (Coarse), **c** C2 (Coarse), **d** F1 (Fine), **e** F2 (Fine), **f** UF (Ultra-fine)

Space discretization was done with the second order centered stabilized "EF_stab" scheme [6] and time discretization with the second order explicit Adams-Bashforth scheme. The wall-adaptive local eddy viscosity (WALE) model [7] was used to model the universal small scale eddies. In cases where the grid resolution near the wall is not of order 1, the Reichardt wall law [5] was used.

Due to the regular pattern of the grid, a constant velocity profile as initial condition was not sufficient to generate turbulence. So a fully developed turbulent flow field from another simulation (on a coarser mesh) was used as initial condition. Periodic boundary condition was applied axially. A momentum source term was added to maintain constant flow rate. Two point correlation coefficient between the velocity component in the streamwise (axial) direction is plotted in Fig. 4. It falls to zero at half a period suggesting that the streamwise domain length is sufficient. No-slip condition was imposed on the inner and outer walls.

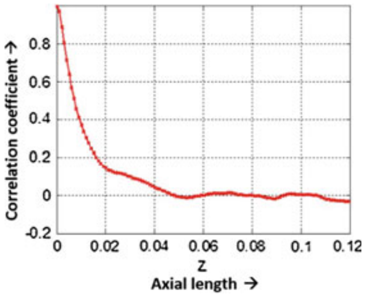

Fig. 4 Two point correlation for streamwise velocity

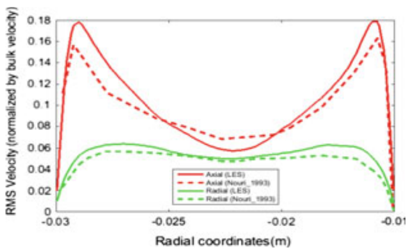

Fig. 5 Standard deviation of velocity for F2 case

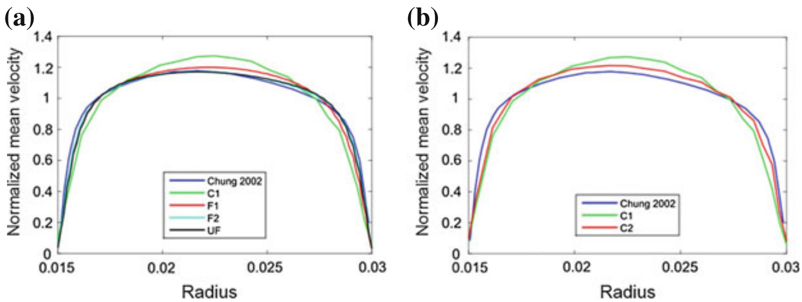

Fig. 6 **a** Comparison for fine meshes, **b** Comparison for coarse meshes

2.1 Results

The turbulent statistics were collected after the flow stabilized. The averaging was done over 25 flow traversals. For the case F2, standard deviation of radial and axial velocity was computed as shown in Fig. 5. It is in good agreement with experimental data of [8]. A comparison of mean velocity profiles for 4 different simulations in Table 1 is presented in Fig. 6a. Comparison of the coarse C1 profile with F1 shows an improvement due to the refinement in all directions. The F2 mesh was created with the same number of elements as F1 but the resolution in azimuth was doubled and that in axial was halved. The profile for F2 agrees well with DNS of [3]. UF mesh also shows similar profile as F2. Hence one could go up to the resolution in wall units of the order of 10 in axial, 3 in azimuthal and 1.3 in radial to reproducing the benchmark result. It should be noted that the total number of elements was maintained for cases F1, F2, UF. The above sensitivity analysis shows that the mean velocity profile has a stronger dependence on azimuthal resolution compared to axial resolution for the 4 said meshes. A similar test was made with the coarse mesh. The azimuthal resolution in C1 was doubled to create C2 mesh. Again, Fig. 6b shows a significant improvement in the profile from C1 to C2.

3 Pressure Fluctuations in an Annular Pipe with a Circular Grid

A realistic PWR core has a square spacer grid. However, creation of a square grid inside an annular pipe would lead to unstructured mesh (at least in its vicinity if we implement hybrid meshing). Since the aim is to understand the physics of the problem, we implemented a circular grid instead. As a result, generation of a fully structured mesh was possible. Also the domain became symmetric. This improved the speed of simulation. In order to make it more realistic, the ratio of hydraulic diameters between the inner and outer flow areas was kept the same for both types of grids. The pipe with the circular grid is shown in Fig. 7. The length of the domain was 0.2688 m, i.e., approximately 9 hydraulic diameters.

Table 2 presents the grid resolutions in different directions. An attempt was made to keep in consideration the acceptable resolutions obtained in Sect. 2.1. However, as seen from Table 2, some compromise had to be made due to lack of computational time and resources. The domain consisted of 20.7 million tetrahedrons and simulation was carried out on 710 parallel processors. All numerical parameters were the same as in Sect. 2 except the boundary conditions at the inlet and outlet. A fully developed

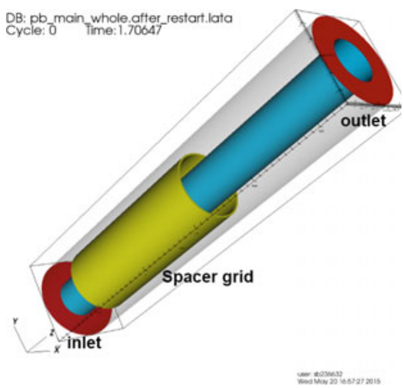

Fig. 7 Annular pipe with circular grid

Table 2 Grid resolution

Direction	Boundary	Grid resolution (in wall units)	Grid resolution (in meters)
Radial	Inner wall	3.2	0.0003
	Outer wall	2.9	0.0003
	Circular grid	3.6	0.0003
Azimuthal	Inner wall	2.8	0.00026
	Outer wall	5.4	0.00055
	Circular grid	4.8	0.0004
Axial	Inner wall	12.9	0.0012
	Outer wall	11.7	0.0012
	Circular grid	14.5	0.0012

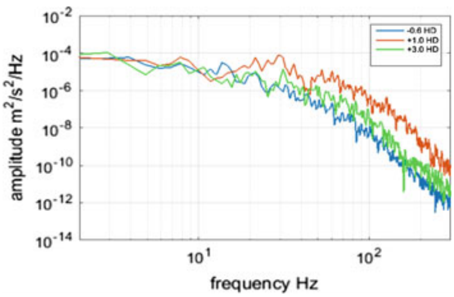

Fig. 8 PSD of instantaneous velocity

turbulent velocity field was injected at the inlet at each time step (from a simultaneous LES). A constant pressure zero was imposed at the outlet.

3.1 Results

Instantaneous velocity fluctuations were analyzed in terms of power spectral density (PSD) at 3 heights: 0.6 HD upstream, 1 HD downstream and 3 HD downstream. Figure 8 shows that the amplitude of fluctuations 1 HD downstream is a decade higher than that upstream. At 3 HD, the amplitude is reduced but still higher than that upstream. This increase in fluctuation is due to the presence of the circular spacer grid. In Fig. 9, the PSD of pressure fluctuations on the inner wall of the pipe shows that the amplitude of fluctuation is higher downstream compared to upstream. The fluctuations or amplitude of power decrease with frequency. Figure 10 shows an angular distribution of standard deviation of the pressure field on the inner wall. The deviation increases by 50% at 1 HD downstream. The symmetric distribution is due to the symmetry of the grid.

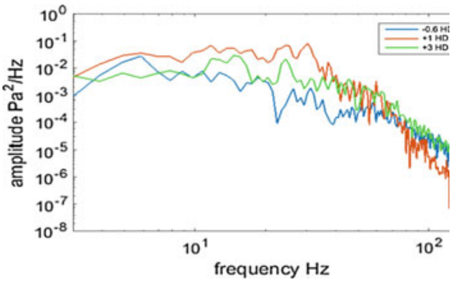

Fig. 9 PSD of pressure fluctuations on the inner wall

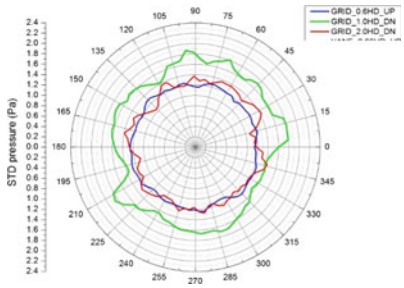

Fig. 10 Angular distribution of standard deviation of pressure on the inner wall

4 Conclusion

A mesh sensitivity analysis with structured grids was performed in an annular pipe using LES. Velocity profiles for 5 different meshes were compared with benchmark DNS, following which an acceptable grid resolution of the order of 10 (axial), 3 (azimuthal) and 1.3 (radial) in wall units was proposed. It was observed that the results are more sensitive to azimuthal resolution than axial resolution. Presence of a circular spacer grid in the pipe increased the fluctuation downstream of the grid as seen from the PSD plots of velocity and wall pressure. As future work, it would be interesting to repeat the same study with a square spacer grid. Also the grid resolutions in Table 2 could be improved to reach the one discussed in Sect. 2.1.

References

1. Bieder, U., Graffard, E.: Qualification of the CFD code Trio_U for full-scale reactor applications. Nucl. Eng. Des. **238**, 671–679 (2008)
2. CCRT-Computing Center for Research and Technology, France. http://www-hpc.cea.fr/en/complexe/tgcc-curie.htm
3. Chung, S.Y., Rhee, G.H., Sung, H.J.: Direct numerical simulation of turbulent concentric annular pipe flow Part 1: Flow field. Int. J. Heat Fluid Flow. **23**, 426–440 (2002)
4. Geuzaine, C., Remacle, J.F.: Gmsh–A three dimensional finite element mesh generator with built-in pre- and post-processing facilities. Int. J. Numer. Methods Eng. **79**, 1309–1331 (2009)
5. Hinze, J.O.: Turbulence. McGraw-Hill, New York (1959)

6. Kuzmin, D., Turek, S.: Multi dimensional FEM-TVD paradigm for convection-dominated flows. Proc. ECCOMAS, Jyvaskyla. 24–28 July, 1–19 (2004)
7. Nicoud, F., Ducros, F.: Sub-grid scale stress modeling based on the square of the velocity gradient tensor. Flow Turbul. combust. **62**, 183–200 (1999)
8. Nouri, J.M., Umur, H., Whitelaw, J.H.: Flow of Newtonian and non-Newtonian fluids in concentric and eccentric annuli. J. Fluid Mech. **253**, 617–641 (1993)
9. Trio_U-Computational Fluid Dynamics code version 1.7.0: French Alternative Energies and Atomic Energy Commission (CEA), France. http://www-trio-u.cea.fr